

Article

Saccharides Emissions from Biomass and Coal Burning in Northwest China and Their Application in Source Contribution Estimation

Kun He ¹, Jian Sun ^{1,*}, Xin Wang ², Bin Zhang ¹, Yue Zhang ¹, Renjian Zhang ³  and Zhenxing Shen ^{1,*} 

¹ Department of Environmental Science and Engineering, Xi'an Jiaotong University, Xi'an 710049, China; k122258604@stu.xjtu.edu.cn (K.H.); zb0825@stu.xjtu.edu.cn (B.Z.); zy403126757@stu.xjtu.edu.cn (Y.Z.)

² School of Chemical and Biomolecular Engineering, Georgia Institute of Technology, Atlanta, GA 30332, USA; xin.wang@chbe.gatech.edu

³ Key Laboratory of Middle Atmosphere and Global Environment Observation, Institute of Atmospheric Physics, Academy of Sciences, Beijing 100029, China; zrj@mail.iap.ac.cn

* Correspondence: sunjian0306@mail.xjtu.edu.cn (J.S.); zxshen@mail.xjtu.edu.cn (Z.S.)

Abstract: Saccharides are important tracers in aerosol source identification but results in different areas varied significantly. In this study, six saccharides (levoglucosan, arabinol, glucose, mannitol, inositol, and sucrose) were determined for their emission factors and diagnostic ratios from domestic combustion of typical biomass and coal fuels in Northwest China. Three types of coal (i.e., anthracitic coal, bituminous coal, and briquettes) and five types of biomass (i.e., maize straw, wheat straw, corn cob, wood branches, and wood block) collected from regional rural areas were selected. Overall, the ranking of the fuel types in terms of the emission factor of particulate matter less than 2.5 μm in diameter ($\text{PM}_{2.5}$) was coal < firewood fuel < straw fuel, with a range of 0.14–36.70 g/kg. Furthermore, the emission factor (e.g., organic carbon (OC) levels) of traditional stove-Heated Kang in the Guanzhong Plain differed significantly from that of wood stoves burning the same fuel, which is attributable to differences in the combustion conditions. The combined diagnostic ratios of levoglucosan (LG)/OC and arabinol/elemental carbon can be used to accurately distinguish the source contribution from coal and biomass combustion to atmospheric PM. Estimation of the biomass burning (BB) contribution to $\text{PM}_{2.5}$ had an uncertainty of -2.7% to 41.0% and overestimation of $9.9\text{--}28.2\%$ when LG was used as the sole tracer, despite its widespread use in other studies; thus, these estimation methods are inadequate and require improvement. The results also revealed that specialized emission control and clean energy strategies are required for both residential BB and non-BB sources on a regional scale.

Keywords: solid fuels; saccharides; source apportionment; contribution bias



Citation: He, K.; Sun, J.; Wang, X.; Zhang, B.; Zhang, Y.; Zhang, R.; Shen, Z. Saccharides Emissions from Biomass and Coal Burning in Northwest China and Their Application in Source Contribution Estimation. *Atmosphere* **2021**, *12*, 821. <https://doi.org/10.3390/atmos12070821>

Academic Editor: Tania Martellini

Received: 14 May 2021

Accepted: 25 June 2021

Published: 27 June 2021

Publisher's Note: MDPI stays neutral with regard to jurisdictional claims in published maps and institutional affiliations.



Copyright: © 2021 by the authors. Licensee MDPI, Basel, Switzerland. This article is an open access article distributed under the terms and conditions of the Creative Commons Attribution (CC BY) license (<https://creativecommons.org/licenses/by/4.0/>).

1. Introduction

Although many areas in China have implemented clean energy transformation plans in recent years, coal and biomass are still major sources of energy for domestic cooking and heating purposes in most rural and suburban areas [1–3]. Combustion activities produce a large amount of particulate matter (PM), the constituent elements of which (e.g., organic carbon (OC), elemental carbon (EC), ions, and saccharides) affect global air quality and human health [4–8]. OC has both primary and secondary origins and includes components, such as polycyclic aromatic hydrocarbons with possible mutagenic and carcinogenic effects [9,10]. EC is formed from the incomplete combustion of carbon-based fuels; its strong light absorption affects the atmospheric chemical reaction process [11,12]. The optical properties and physical and chemical processes of the atmosphere are also affected by ion concentrations [13,14]. Saccharides are a major class of water-soluble organic compounds in atmospheric aerosols, which affect the hygroscopic properties of particles. Some saccharides, such as levoglucosan (LG), can be used as tracer because of its source (cellulose or hemicelluloses thermal degradation) and relatively stability in

the atmospheric environment [15–20]. A deeper understanding of the characteristics of PM_{2.5} and its composition is vital for investigating the causes and influential factors in the atmospheric environment and implementing measures for improvement of accuracy and reliability.

LG (1,6-anhydro-β-D-glucopyranose) is a specific marker of biomass burning aerosols because of its source-specific generation and atmospheric stability [21–23]. Several studies have utilized LG to estimate the BB contribution to OC and PM less than 2.5 μm in diameter (PM_{2.5}) in specific regions [24–28]. For example, an early Beijing study determined that BB contributions ranged from 18% to 38% in PM_{2.5} and accounted for approximately 14% to 32% of the PM₁₀ in the aerosol background component [29]. Wang et al. [30] recorded that the BB/OC and BB/PM_{2.5} ratios in atmospheric aerosols in wintertime of Xi'an, the largest city in northwest China, were 32.4% and 16.0%. Studies have typically measured LG because it is often the only or most identifiable indicator of BB. However, some studies reported that non-BB sources (such as solid waste burning, fireworks burning, meat cooking, and coal combustion (CC)) also emitted LG as BB did [31–36]. Among the non-BB sources, coal combustion may have crucial impacts on LG emissions in China due to its large consumption in energy supply structure. LG may be present in coal combustion emissions because coal is formed through geologic processes and some coals may have cellulose remnants [33,35]. Therefore, using LG alone to evaluate the contribution of biomass combustion to the environment leads to overestimation and inaccuracy. Wu et al. [32] determined that local BB contributions have been substantially overestimated by 4.28–369% in previous studies that used LG as their sole BB source. However, LG emissions varied across regions because of the varying industrial and energy structures; this uncertainty in the emission inventory of different regions is also a challenge to measuring BB contribution. Therefore, a reevaluation of potential emission sources of LG and its effect on the original BB contribution method must be conducted and is crucial for understanding the pollution factor and formulating local countermeasures.

The goals of this study were to identify comprehensive emission characteristics of typical biomass and coal fuel in Northern China, as well as deviations with the BB estimation method. To achieve these goals, the OC/EC, ions, and saccharides of common biomass and coal fuel samples under different burning conditions were measured in Northwest China, which is still affected by heavy BB and CC pollution in winter [30,37,38]. In this study, the source-specific emission factor (EF) and diagnostic ratio between components in biomass and coal were compared. In addition, the total LG emission from CC and BB in Shaanxi Province was estimated, and the influence of combustion conditions and evaluation method on source contribution was also assessed.

2. Methodology

2.1. Fuel and Stove

The samples were collected in rural field studies, with the sampling points located in the east, west, and middle of the Guanzhong Plain. These locations contained typical fuels used in rural areas of Northwest China. Eight selected fuels were categorized into two groups, namely coal (anthracitic coal, bituminous coal, and briquettes) and biomass (corn cob, maize straw, wheat straw, wood branches, and wood blocks). The briquettes used in this study were mostly made from anthracitic coal. These fuels were further subjected to proximate analysis to determine their moisture level, ash content, volatile matter content, and heat value, which are listed in Table 1 (on an as-received basis). Both biomass and coal fuel come from the local users for heating and cooking, and are representative. The combustion conditions in this study were the real usage conditions of the materials by local residents and could be divided into coal (coal stove) and biomass (wood stove and Heated Kang) groups. The sampling information and combustion conditions are listed in Appendix A Table A1. The traditional stove-Heated Kang is used for heating and has a long history of usage in rural areas of the Guanzhong Plain; a detailed structure of this stove is provided in Figure 1, and its characteristics are described in our previous publication [39].

The air inlet was limited to the small hole in the feed inlet which was aimed to extend the combustion time and, thus, get a slow-release effect of heat for space heating, and the oxygen supply is, thus, insufficient.

Table 1. Proximate analysis of coal and biomass fuels.

Fuel Types	Moisture, %	Ash, %	Volatile Matter, %	Fixed Carbon, %	Heating Value, MJ/kg
Anthracitic Coal	0.88	9.72	6.12	83.28	29.68
Bituminous Coal	7.98	7.98	33.20	50.84	22.02
Briquettes	3.00	32.34	4.99	59.67	20.37
Corn Cob	4.87	5.93	71.95	17.25	17.72
Wood Branches	4.39	2.15	82.96	10.51	18.03
Wood Block	4.39	2.15	82.96	10.51	18.03
Maize Straw	6.10	4.70	76.00	13.20	17.73
Wheat Straw	4.39	8.90	67.36	19.32	14.52

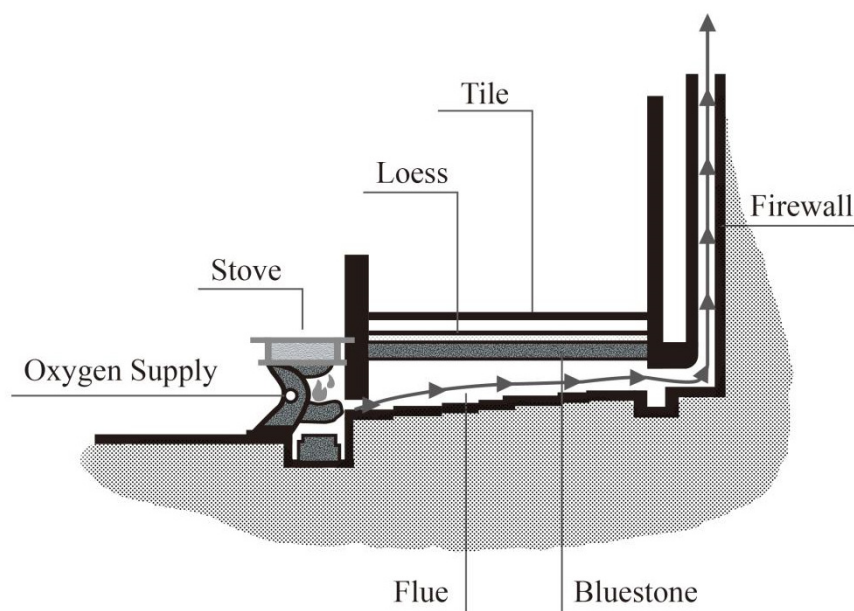


Figure 1. Schematic diagram of the structure of Heated Kang.

2.2. Sample Collection

A dilution sampling system was used for flue gas collection in this study, in which the dilution ratio could be adjusted 5–50 times. This device was designed and manufactured by the Desert Research Institution (Reno, NV, USA), and the specific structure is depicted in Figure 2.

PM_{2.5} samples were collected from three parallel channels located downstream of the residence chamber at a flow rate of 5 L/min. Two channels equipped with 47-mm quartz filters (Whatman, Maidstone, Kent, UK) and another equipped with a 47-mm Teflon filter (Pall Life Sciences, Ann Arbor, MI, USA) were used. The filters were weighed before and after sampling on a microbalance ($\pm 1 \mu\text{g}$ precision, Sartorius AG MC5; Göttingen, Germany) to obtain the PM_{2.5} mass. Equal gas velocity in sampling probe and stack were set initially and the vertical arrangement of sampling probe and chimney (Figure 2) both guaranteed isokinetic conditions in this study. The extraction velocity was monitored by a flowmeter (TSI 3031, Shoreview, MN, USA). The dilution air has been dried and filtrated to guarantee a dry and clean condition; and a dilution ratio over 10 in this study could guarantee an acceptable humidity (<40%) and temperature (<25 °C) for the final exhaust. The PM_{2.5} sample collection efficiency was based on the design of PM_{2.5} impactor (Airmetrics, Eugene, OR, USA), which has been widely employed in this field. A standard flow rate would technically guarantee the PM_{2.5} cutting efficiency. The mass concentration

of each sample filter was obtained through subtraction from the field blank to eliminate any passive gas adsorption artifacts.

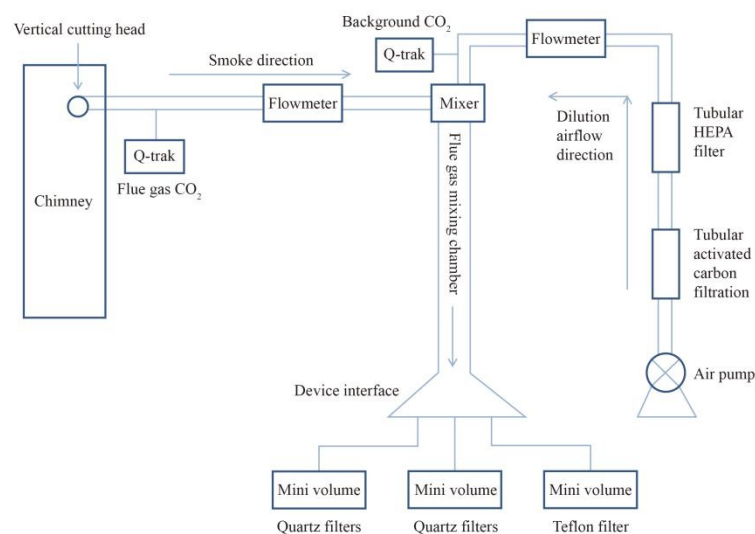


Figure 2. Structure diagram of flue gas collection device.

2.3. Chemical Analysis

OC/EC analysis: OC and EC were quantified on the basis of a punch (0.526 cm^2) from the quartz-fiber filter through the use of the thermal optical reflectance technique with a thermal/optical carbon analyzer (DRI Model, 2001; Atmoslytic, Calabasas, CA, USA) and the IMPROVE_A protocol ($\text{TC} = \text{EC} + \text{EC}$, $\text{OC} = \text{OC1} + \text{OC2} + \text{OC3} + \text{OC4} + \text{OP}$, $\text{EC} = \text{EC1} + \text{EC2} + \text{EC3} - \text{OP}$) [40]. The punch (0.526 cm^2) is heated in an oxygen-free pure He environment, setting the heating gradient to $140 \text{ }^\circ\text{C}$ (OC1), $280 \text{ }^\circ\text{C}$ (OC2), $480 \text{ }^\circ\text{C}$ (OC3), and $580 \text{ }^\circ\text{C}$ (OC4). In this process, the particulate organic carbon on the filter is burned to generate CO_2 ; the second stage of the sample is heated in an environment of 2% oxygen and helium, and the heating gradient is $580 \text{ }^\circ\text{C}$ (EC1), $740 \text{ }^\circ\text{C}$ (EC2), and $840 \text{ }^\circ\text{C}$ (EC3). At this time, elemental carbon is oxidized to CO_2 in this process. The CO_2 generated under various temperature gradients is reduced to methane by MnO_2 in the reduction furnace, and its concentration can be detected by the flame ion detector. Due to the coking effect produced during the heating process of the sample, some organic carbon will undergo a cracking reaction to form Pyrolysis Organic Carbon (OP). It is necessary to use a He/Ne laser with a wavelength of 633 nm to irradiate the sample under test. When the intensity change of the reflected light and transmitted light of the filter film returns to the initial value, the starting point of elemental carbon oxidation can be determined, that is, OP is returned to the OC part, and the organic carbon and elemental carbon concentration values are finally determined. The EC and OC concentrations in the sample sets were all above the detection limit (0.01 and $0.39 \text{ } \mu\text{g cm}^{-2}$, respectively).

Water-soluble inorganic ion analysis: One-quarter of the quartz-fiber filter was extracted with deionized water (10 mL), and the extractants were filtered through microporous membranes ($0.45 \text{ } \mu\text{m}$ pore size) to remove insoluble materials. Eight inorganic ions were analyzed through Dionex ion chromatography (DX-600; Sunnyvale, CA, USA). The detection limits of Na^+ , NH_4^+ , K^+ , Mg^{2+} , Ca^{2+} , Cl^- , NO_3^- , and SO_4^{2-} were 4.6 , 4.0 , 10.0 , 4.0 , 5.0 , 20.0 , 15.0 , and 0.5 ppb , respectively. The chemical analysis procedures were discussed by Shen et al. [41].

Saccharides analysis: One-half of each quartz-fiber filter was extracted with high-purity dichloromethane and methanol ($2:1$, v/v) under ultrasonication for 15 min . The procedure was repeated three times to ensure complete extraction. The solution was then passed through Pasteur pipettes filled with sodium sulfate (Na_2SO_4) and glass wool to remove water and debris from the combined extracts. A rotary evaporator under vacuum was used to concentrate the extracts to 1 mL . Aliquots of the extracts were reacted with

N,O-bis-(trimethylsilyl)trifluoroacetamide (BSTFA) containing 1% trimethylchlorosilane and pyridine at 70 °C for 3 h. After the solution is cooled, add 40 µL internal standard (hexamethylbenzene, 1.512 ng. µL⁻¹), mix well, and place in the refrigerator for testing. The silanization reaction of BSTFA can convert polar groups, such as hydroxyl groups of sugars into non-polar groups, which can be detected by gas chromatography/mass spectrometer (GC/MS) (7890A/5975C; Agilent Technologies, Santa Clara, CA, USA). One microliter of the reactant was injected into a GC/MS. The extract was injected through a GC injection port at 275 °C in an auto-sampler, and the GC separation made use of a DB-5MS fused-silica capillary column (30 m × 0.25 mm i.d., 0.25 µm film thickness, Agilent Technology). The MS was operated in the selective ion monitoring mode (SIM) with two ions monitored for each compound and dwell times ranging between 25 and 50 ms. The GC oven was programmed to increase from room temperature to 50 °C in 2 min, ramped to 120 °C (at a rate of 15 °C min⁻¹), then to 300 °C (at 5 °C min⁻¹), and, finally, held at 300 °C for 16 min. The target compounds were identified by comparison of their retention times and ratios of qualifier ions with those in standards. An Internal standard (IS) was added into the samples to qualify the actual amounts of the target compounds. In this study, the detection method was designed to measure saccharides, n-alkanes, and PAHs at the same time [42], resulting in pretty busy peaks in the GC/MS curve. In addition, the relatively great gap between LG and MA (GA) concentrations makes it hard to identify the small peaks of GA and MA. Therefore, these two species of saccharides were rarely detected in this study. The recoveries of organic compounds ranged from 70 to 130%, and all concentrations reported in this study were recovery and blank corrected. In addition, the concentration of LG and arabitol in source can be calculated based on their EF and stove volume (15–25 L), and details can be found in the Support Information. The concentration of LG and arabitol in stove was far greater than that in ambient [30]; thus, the ambient background can be ignored.

2.4. Data Processing

The EF is defined as the amount of pollutants emitted from a unit weight of fuel burned (on an as-received basis) [43,44] and is calculated as follows [45]:

$$EF_p = \frac{V_{\text{Total-chimney}}}{m_{\text{fuel}}} \frac{m_{\text{filter}}}{Q} DR, \quad (1)$$

where $V_{\text{Total-chimney}}$ is the total volume of exhaust flowing through the chimney during the experiment (m³) at a standard temperature and pressure, m_{fuel} is the mass of the burned fuel (kg), m_{filter} is the mass of pollutants collected on the filter (g), Q is the sampling volume through the filter (m³), and DR is the dilution rate of the dilution sampling system. DR can be calculated as follows:

$$\text{Flow – based } DR = Q_t / Q_{in} \quad (2)$$

Because the dilution channel used in the field experiment does not have real-time CO₂ concentration monitoring, its dilution factor was calculated from the flow rate of the three nodes, namely the flue gas intake Q_{in} , the dilution gas volume Q_{di} , and the diluted total gas volume Q_t ($Q_t = Q_{in} + Q_{di}$).

3. Results and Discussion

3.1. General Description of PM_{2.5} EFs

The statistical results of PM_{2.5} and main component EFs collected from biomass and coal in different combustion conditions are presented in Table 2. Overall, the ranking of the fuel types in terms of their EFs of PM_{2.5} was coal < firewood fuel < straw fuel, with a range of 0.14–36.70 g/kg. The EF of PM_{2.5} in bituminous coal was an exception, with an almost 200 times higher EF than that of anthracitic coal, which can be attributed to the high volatile content in bitumite [46,47]. The difference in the PM_{2.5} EFs between anthracitic coal and briquettes was nonsignificant because the main material of briquettes used in this study

was anthracitic coal. The maize straw burning in the Heated Kang yielded the highest $PM_{2.5}$ EF (36.70 ± 4.12 g/kg), which was an order of magnitude higher than that recorded in the literature (2.45–8.18 g/kg) on account of its unique combustion conditions [48–50]. The stove structure also affects the combustion conditions [51], and Figure 1 depicts the oxygen supply in Heated Kang; it is deficient because of the windshield structure with small holes; thus, combustible PM cannot be fully oxidized before discharge [39,52]. In addition, a result of oxygen-deficient combustion, the OC emissions from straw in Heated Kang were significantly higher than those from the other fuel–stove combinations. The EFs of OC reached 20.65 ± 1.14 g/kg and 10.43 ± 1.79 g/kg for maize straw and wheat straw, respectively, which were also higher than those reported in the literature (0.85–3.21 g/kg) [53]. The EFs of $PM_{2.5}$ and OC in a firewood stove were lower than those in Heated Kang, but the EFs of EC exhibited a reverse sequence, likely due to the better ventilation and higher combustion temperature in firewood stoves than in Heated Kang [52]. Similar to their ranking in terms of EFs of $PM_{2.5}$, the fuel types were ranked as follows according to their EFs of water-soluble ions: coal < firewood fuel < straw fuel, though with much lower concentrations (2.93–8.94%) compared with the concentrations of total carbon (32.56–71.71%). These results are consistent with those reported in the literature [54,55], indicating that the $PM_{2.5}$ emitted from household solid fuel combustion is primarily from carbon-containing substances, especially the high proportion of organic matter. Among the measured ions, that with the highest EF in coal was SO_4^{2-} , with a range of 3.22–300.08 mg/kg, and the anion and cation ions in biomass with the highest EFs were Cl^- and K^+ , respectively. Measurements of Cl^- and K^+ were higher in herbaceous fuels (corn cob, maize straw, and wheat straw) than in woody fuels (wood branches and wood blocks) [56], which could explain the different EFs of these two ions in straw and wood burning.

The EFs of saccharides, including LG, arabinol, glucose, mannitol, inositol, and sucrose, are listed in Table 2. The range of saccharide EFs for straw fuel was 315.50–434.68 mg/kg, which was higher than that for firewood fuel (104.92–274.70 mg/kg), both of which were three orders of magnitude higher than that of the saccharide EFs from coal combustion. The proportion of LG and arabinol in saccharides were the highest, collectively contributing more than 90% of the total saccharides. In terms of the high OC emission from biomass fuels, we further explored the concentrations of saccharides in OC (Table 3). The saccharide concentration in OC for coal was 0.04‰–14.33‰ and for biomass was 21.05‰–62.00‰. Considering the large consumption of bituminous coal, the total saccharide emission from coal combustion was nonnegligible. Furthermore, the proportion of LG in the OC for coal was 0.02‰–5.33‰, and for biomass was 12.55‰–27.12‰. It is noticed that arabinol was also highly abundant in BB derived $PM_{2.5}$ which proportions in OC showed even significant difference between biomass and coal. Solid fuel combustion sources (e.g., biomass, coal, etc.) existed in the atmosphere when the proportion of LG (arabinol) in $PM_{2.5}$ OC was greater than zero. In addition, the BB contribution could be deduced, when the ratios of LG/OC and arabinol/OC were greater than 14.58‰ and 8.20‰, respectively. Considering that other saccharides may be hydrolyzed or converted from other effects (e.g., photosynthesis), LG is still undeniably an accurate indicator of saccharides in the initial inference of source, although studies have determined that LG is not solely derived from biomass and coal. However, arabinol has not yet been widely used in source identification.

Table 2. Emission factors of various substances of fuel under different combustion conditions.

Species	Unit	Coal Stove			Wood Stove			Heated Kang			
		Anthracitic Coal	Bituminous Coal	Briquettes	Corn Cob	Wood Branches	Wood Branches	Wood Block	Maize Straw	Wheat Straw	
PM _{2.5}	g/kg	0.14 ± 0.02	26.80 ± 1.13	0.43 ± 0.03	17.77 ± 3.18	9.09 space ± space 1.52		14.87 ± 0.54	7.07 ± 1.20	36.70 ± 4.12	25.63 ± 1.28
OC	g/kg	0.03 ± 0.02	5.16 ± 1.87	0.12 ± 0.02	7.49 ± 2.42	2.87 ± 0.47		6.63 ± 1.72	4.13 ± 0.46	20.65 ± 1.14	10.43 ± 1.79
EC	g/kg	0.02 ± 0.00	7.36 ± 2.24	0.02 ± 0.01	4.21 ± 0.08	2.32 ± 0.19		1.26 ± 0.21	0.95 ± 0.06	3.88 ± 0.31	0.70 ± 0.14
TC	g/kg	0.05 ± 0.02	12.52 ± 0.37	0.14 ± 0.02	11.69 ± 2.34	5.19 ± 0.66		7.89 ± 1.93	5.07 ± 0.51	24.53 ± 1.46	11.13 ± 1.93
OC1	g/kg	0.01 ± 0.01	0.81 ± 0.30	0.04 ± 0.01	1.51 ± 0.72	0.59 ± 0.16		2.89 ± 0.88	1.85 ± 0.28	10.96 ± 0.25	6.23 ± 2.00
OC2	g/kg	0.01 ± 0.00	1.53 ± 0.36	0.03 ± 0.00	1.21 ± 0.79	0.35 ± 0.02		1.72 ± 0.08	1.19 ± 0.09	5.38 ± 0.38	2.15 ± 0.15
OC3	g/kg	0.01 ± 0.00	1.57 ± 0.74	0.04 ± 0.01	2.60 ± 1.64	0.99 ± 0.09		1.24 ± 0.77	0.54 ± 0.00	2.31 ± 0.18	0.91 ± 0.11
OC4	g/kg	ND	1.78 ± 0.77	0.01 ± 0.00	1.16 ± 0.07	0.60 ± 0.08		0.24 ± 0.11	0.07 ± 0.05	0.30 ± 0.05	0.11 ± 0.03
EC1	g/kg	0.01 ± 0.00	4.05 ± 1.19	0.01 ± 0.01	5.20 ± 0.88	2.61 ± 0.30		1.77 ± 0.08	1.41 ± 0.08	5.56 ± 0.58	1.71 ± 0.24
EC2	g/kg	0.01 ± 0.00	3.18 ± 0.98	0.01 ± 0.00	0.01 ± 0.01	0.04 ± 0.03		0.01 ± 0.01	0.01 ± 0.00	0.02 ± 0.00	0.01 ± 0.01
EC3	g/kg	ND	0.13 ± 0.07	ND	ND	0.01 ± 0.02		0.01 ± 0.00	ND	0.01 ± 0.00	ND
OP	g/kg	ND	-0.52 ± 0.30	ND	1.01 ± 0.79	0.34 ± 0.17		0.54 ± 0.12	0.47 ± 0.03	1.70 ± 0.27	1.02 ± 0.08
Na ⁺	mg/kg	1.72 ± 0.07	28.11 ± 30.14	9.53 ± 0.32	22.46 ± 1.15	66.91 ± 58.54		92.81 ± 44.81	40.06 ± 0.30	168.42 ± 156.61	46.72 ± 16.16
NH ₄ ⁺	mg/kg	0.66 ± 0.76	64.71 ± 9.17	0.46 ± 0.20	12.15 ± 14.72	21.49 ± 0.33		78.28 ± 11.08	20.61 ± 12.07	45.15 ± 38.20	377.16 ± 386.67
K ⁺	mg/kg	0.30 ± 0.02	62.53 ± 49.17	1.04 ± 0.10	754.81 ± 138.37	371.34 ± 213.21		155.03 ± 100.81	56.57 ± 19.86	381.84 ± 187.84	263.85 ± 34.90
Mg ²⁺	mg/kg	0.11 ± 0.02	7.67 ± 0.27	0.74 ± 0.00	1.68 ± 0.04	4.60 ± 4.17		7.22 ± 3.93	3.21 ± 1.06	4.47 ± 2.61	3.82 ± 2.75
Ca ²⁺	mg/kg	1.11 ± 0.10	68.39 ± 18.03	7.75 ± 0.25	17.08 ± 6.92	57.53 ± 46.91		133.15 ± 64.39	62.08 ± 1.97	117.66 ± 46.26	78.38 ± 27.59
Cl ⁻	mg/kg	0.38 ± 0.08	224.72 ± 132.04	0.97 ± 0.33	458.56 ± 153.89	178.81 ± 82.62		160.18 ± 148.27	27.84 ± 2.66	222.00 ± 6.16	764.84 ± 772.10
NO ₃ ⁻	mg/kg	0.89 ± 0.19	76.55 ± 27.08	5.85 ± 1.74	5.61 ± 1.92	19.20 ± 15.19		38.40 ± 15.62	14.37 ± 5.32	17.58 ± 1.83	14.00 ± 2.62
SO ₄ ²⁻	mg/kg	3.22 ± 1.22	300.08 ± 212.40	3.96 ± 5.61	48.79 ± 15.8	92.91 ± 61.53		180.61 ± 71.69	63.15 ± 19.35	116.98 ± 31.22	261.46 ± 156.33
Levogluconan	mg/kg	0.16 ± 0.23	0.08 ± 0.03	0.34 ± 0.47	126.60 ± 33.34	41.84 ± 19.24		123.34 ± 29.95	111.99 ± 50.76	259.20 ± 32.93	165.54 ± 2.94
Arabitol	mg/kg	0.24 ± 0.34	0.11 ± 0.03	0.12 ± 0.02	188.24 ± 50.00	62.34 ± 29.71		150.24 ± 3.12	143.93 ± 50.48	169.42 ± 216.42	164.00 ± 68.42
Glucose	mg/kg	ND	ND	ND	ND	ND		ND	ND	2.85 ± 4.03	0.06 ± 0.08
Mannitol	mg/kg	ND	ND	ND	ND	ND		0.20 ± 0.28	ND	ND	0.12 ± 0.16
Inositol	mg/kg	ND	ND	ND	ND	ND		ND	ND	1.05 ± 0.11	0.12 ± 0.16
Sucrose	mg/kg	0.03 ± 0.04	ND	0.13 ± 0.19	0.66 ± 0.09	0.74 ± 0.01		0.92 ± 0.60	0.16 ± 0.02	2.16 ± 0.38	39.73 ± 5.69
Total Saccharides *	mg/kg	0.43 ± 0.61	0.19 ± 0.03	0.59 ± 0.66	315.50 ± 83.43	104.92 ± 48.96		274.70 ± 33.95	256.08 ± 101.26	434.68 ± 244.83	369.57 ± 65.92

Note: ND denotes not detected. TC: total carbon. The data are shown as mean ± standard deviation. * denotes the sum of levoglucosan, arabitol, glucose, mannitol, inositol, and sucrose.

Table 3. Saccharides/OC and LG/OC of fuel under different combustion conditions (‰).

Ratio	Coal Stove			Wood Stove			Heated Kang		
	Anthracitic Coal	Bituminous Coal	Briquettes	Corn Cob	Wood Branches	Wood Branches	Wood Block	Maize Straw	Wheat Straw
Saccharides/OC	14.33	0.04	4.92	42.12	36.56	41.43	62.00	21.05	35.43
LG/OC	5.33	0.02	2.83	16.90	14.58	18.60	27.12	12.55	15.87
Arabitol/OC	8.00	0.02	1.00	25.13	21.72	22.66	34.85	8.20	15.72

3.2. Comparison of Diagnostic Ratios of PM_{2.5} between BB and CC

To better systematically distinguish between different sources of PM_{2.5}, the proportions of specific PM_{2.5} components were calculated, as detailed in Table 4. The use of specific markers and diagnostic ratios of selected individual components is a common method for source identification and apportionment [31]. The OC/EC ratio is a common diagnostic ratio used in PM_{2.5} research to determine basic information regarding its main sources [49,57]. The OC/EC ranges of coal, straw fuel, and firewood fuel in this study were 0.70–6.00, 1.78–14.90, and 1.24–5.26, respectively, and were slightly higher than those previously reported in the literature [53,58,59]. The OC/EC ratios in anthracite (1.50) and briquettes (6.00) were far greater than that in bituminous coal (0.70), indicating that coal form and quality influence OC and EC emissions [60]. The OC/EC ratio in Heated Kang was higher than that in firewood stoves because of the greater production of OC in oxygen-deficient environments. In addition, because of their relatively low combustion temperatures, Heated Kang tended to generate less EC than did firewood stoves [39]. The SO₄²⁻/K⁺ ratio in straw fuel and firewood was 0.06–0.99 and 0.25–1.12 and was much smaller than that in coal (3.81–10.73). This is because biomass combustion emits a large concentration of K⁺ but less SO₄²⁻, resulting in a significantly lower ratio than in CC and other sources (e.g., firework burning: 2.1–4.8); therefore, the SO₄²⁻/K⁺ ratio can be used to identify biomass combustion sources [61]. The difference in K⁺/OC ratio between biomass fuel and coal was not significant, but a difference was observed in the order of magnitude of emissions between Heated Kang (0.01–0.03) and wood stoves (0.10–0.13), indicating that different ventilation conditions affected the diagnostic ratio of K⁺/OC. The K⁺/EC ratio exhibited obvious differences between coal (0.01–0.05) and biomass fuel (0.06–0.38), especially the K⁺/EC ratio of wheat straw in Heated Kang, which was significantly greater than that for other fuels. This phenomenon can be attributed to straw containing more K⁺ than firewood and coal, which can be used as a key parameter in distinguishing the emissions of straw, firewood, and coal combustion [54,62,63].

Table 4. The ratio of specific components for coal and biomass fuel.

Ratio	Coal Stove			Wood Stove			Heated Kang		
	Anthracitic Coal	Bituminous Coal	Briquettes	Corn Cob	Wood Branches	Wood Branches	Wood Block	Maize Straw	Wheat Straw
OC/EC	1.50	0.70	6.00	1.78	1.24	5.26	4.35	5.32	14.90
TC/PM _{2.5}	0.36	0.47	0.33	0.66	0.57	0.53	0.72	0.67	0.43
NO ₃ ⁻ /SO ₄ ²⁻	0.28	0.26	1.48	0.11	0.21	0.21	0.23	0.15	0.05
SO ₄ ²⁻ /K ⁺	10.73	4.80	3.81	0.06	0.25	1.17	1.12	0.31	0.99
K ⁺ /OC	0.01	0.01	0.01	0.10	0.13	0.02	0.01	0.02	0.03
K ⁺ /EC	0.02	0.01	0.05	0.18	0.16	0.12	0.06	0.10	0.38
K ⁺ /LG	1.88	781.63	3.06	5.96	8.88	1.26	0.51	1.47	1.59
SO ₄ ²⁻ /LG	20.13	3751.00	11.65	0.39	2.22	1.46	0.56	0.45	1.58
NO ₃ ⁻ /LG	5.56	956.88	17.21	0.04	0.46	0.31	0.13	0.07	0.08
LG/TC * 1000	3.20	0.01	2.43	10.83	8.06	15.63	22.09	10.57	14.87
LG/OC * 1000	5.33	0.02	2.83	16.90	14.58	18.60	27.12	12.55	15.87
LG/EC * 1000	8.00	0.01	17.00	30.07	18.03	97.89	117.88	66.80	236.49
Arabitol/OC * 1000	8.00	0.02	1.00	25.13	21.72	22.66	34.85	8.20	15.72
Arabitol/EC * 1000	12.00	0.01	6.00	44.71	26.87	119.24	151.51	43.66	234.29

Both biomass burning and coal combustion produced saccharides; thus, the ratio of some saccharides to certain components was calculated to identify the different sources. To ensure a more comparative result, we increased the ratio of saccharides to other components by a factor of 1000. The LG/OC ratio in coal was 0.02–5.33, which was almost one-tenth of that in the biomass fuel (12.55–27.12); thus, the LG/OC ratio is a reliable indicator and distinguisher. Although the difference in LG/EC ratio between coal (0.01–17.00) and biomass (18.03–236.49) was also large, their scope too close to distinguish between these two sources. Similarly, the ranges of the arabitol/OC ratio in coal (0.02–8.00) and biomass (8.20–34.85) almost overlapped, but the difference in arabitol/EC ratio between

coal (0.01–12.00) and biomass (26.87–234.29) reveals the potential of the arabitol/EC ratio for distinguishing between the combustion sources of coal and biomass. An extreme ratio was observed in K^+/LG , SO_4^{2-}/LG , and NO_3^-/LG due to the combination of extremely high ion emissions and low LG emissions; therefore, they could act as potential tracers of bituminous coal among numerous fuels. High K^+/LG ratios were generally associated with low LG/TC ratios, possibly because LG can be broken down under high temperatures but K^+ cannot [62]. Thus, a higher K^+/LG ratio may indicate the predominance of a burning condition.

3.3. Assessment of Present BB Source Contribution Estimation Methods

In addition to clarifying the factors and specific ratios of biomass and coal fuels, some saccharide molecular markers, such as LG, are often used to estimate the contribution of specific sources to the aerosol particle mass [24–28]. Because LG forms in relatively large amounts, is sufficiently stable, and is specific to cellulose-containing substances, it serves as an ideal molecular marker for BB. Notably, the relative contribution of LG to the PM and OC concentrations was dependent on combustion conditions and the fuel itself. In this study, taking the ambient data of Xi'an in 2015 as an example [30], we calculated the contribution of BB to ambient $PM_{2.5}$ by using equations, such as the following:

$$BB/PM_{2.5} = \frac{(LG/PM_{2.5})_{\text{ambient}}}{(LG/PM_{2.5})_{\text{source}}} \quad (3)$$

The ratios of LG to $PM_{2.5}$ emitted from BB were 0.007–0.228 in the literature and 0.007 in this study (Table 5). The results indicated that the contribution of BB to $PM_{2.5}$ was significantly different (1.4–45.1% and 42.4%, respectively) when different source data were used along with the same environmental data. Inducing uncertainty in the BB activity data, EF also varied considerably under different combustion conditions and fuel types. Therefore, selecting an appropriate source ratio, such as the local source ratio, is paramount for reducing this uncertainty and enhancing the accuracy of the BB contribution results. An increasing number of studies have proposed that LG originates not only from BB but also from municipal solid waste burning, firework burning, meat cooking, and coal burning [32,64], drawing attention to the clear overestimation of a single source that has long been overlooked in other studies.

Table 5. The contribution of BB to $PM_{2.5}$ under different source ratios.

Ratio	Fuel types	Source	Ambient ^a	BB/ $PM_{2.5}$	Reference
LG/ $PM_{2.5}$	straw/wood	0.007		42.4%	this study
	crop straw/wood	0.020	0.003	15.8%	Yan et al. 2018
	cereal straw	0.045		7.0%	Zhang et al. 2007
	woods	0.007–0.228		1.4–45.1%	Fine et al. 2004a; Fine et al. 2004b

Note: a means taking the environmental data of Xi'an in 2015 as an example.

Using coal as an example, LG may be detected in coal combustion emissions and coal is the main fuel for energy supply in China. This study demonstrated that the concentration of LG in CC-derived $PM_{2.5}$ was low; however, considering its large consumption of coal in China, the contribution of CC to LG emissions cannot be ignored. We estimated respective LG emissions on the basis of the usage of coal and biomass listed in the 2020 Statistical Yearbook of Shaanxi Province, China. The total consumption of biomass fuels for burning was calculated as

$$M_b = P \times R \times D \times H \times C, \quad (4)$$

where M_b is the dry mass of the biomass used in residential combustion (in t), P is the total production of crops (in t), R is the residue-to-crop ratio, D is the dry fraction of crop residue, H is the harvest residue fraction, and C is the ratio of the fuel consumed through residential combustion. Specific biomass parameters were detailed by Sun et al. [45]. The

results revealed that the estimated emissions of LG from coal, corn crop, wheat crop, and wood burning were 1617.37, 36002.62, 21126.82, and 12915.23 t, respectively. The ratio of biomass (70044.47 t) to coal (1617.37 t) in LG emissions was 43.3, which is strongly consistent with the ratio (45.9) reported by Wu et al. [32] (shown in Table 6). This result demonstrates the relative accuracy of the estimates and the nonnegligibility of non-biomass sources in the Northwest China. The contribution of BB to ambient PM_{2.5} in Xi'an in 2015 was 42.4% when only biomass was considered as the sole source of emissions for LG. However, non-BB sources, including municipal solid waste burning (9.7%), firework burning (9.6%), meat cooking (5.4%), domestic coal burning (1.5%), ritual item burning (0.2%), and industrial coal burning (0.1%), contributed 26.5% of the total LG emissions in China, as recorded by Wu et al. [32]. The influence of coal was not considered, and the contribution of BB in Xi'an to PM_{2.5} was, thus, overestimated by 0.6–1.7%. Because estimation was based on coal burning, the contribution of BB from non-biomass sources in Xi'an to PM_{2.5} was overestimated by 9.9–28.2%; the actual contribution of BB to PM_{2.5} is approximately 14.2–32.5%. Therefore, local BB contributions have been substantially overestimated in previous studies, wherein LG was identified as the sole BB source. A reassessment of LG emissions from BB and non-BB sources and estimation methods is urgently required to eliminate remaining biases or errors for future estimations of the effect of BB on aerosols.

Table 6. Estimated LG emissions of biomass and coal in Shaanxi Province in 2019.

Fuel	Yield/10 ⁴ t	Consumption ^a /10 ⁴ t	EF-LG ^b /(mg/kg)	Estimated Emission/t	Biomass/Coal
Coal	13478.06	13478.06	0.12	1617.37	
Corn Crops	609.58	93.32	385.80	36002.62	
Wheat Crops	382.04	127.62	165.54	21126.82	43.3
Woods	460.93	132.75	97.29	12915.03	

Note: a: actual consumption of biomass fuel calculated by (2). b: estimated emission factors for each fuel (Coal: the average value of anthracitic coal and bituminous coal; Corn Crops: the sum of corn cob and maize straw; Wheat Crops: the EF of wheat straw; Woods: the average value of wood branches and wood block).

4. Conclusions

In this study, typical biomass and coal fuels were selected to investigate emission characteristics and diagnostic ratios. We evaluated the widely used source apportionment method that considers BB as the sole source of LG and identified a high level of uncertainty in its veracity. Overall, the fuel types were ranked as follows according to their EFs of PM_{2.5}: coal < firewood fuel < straw fuel. Fuel types and combustion conditions both strongly affected the EFs of PM_{2.5} and the main chemical components. The LG/OC and arabitol/EC ratios can serve as suitable indicators to distinguish sources of CC and BB; however, these diagnostic ratios also varied under different combustion conditions. Other studies have typically used LG to estimate the contribution of BB to PM_{2.5} and OC contents in urban sites. Uncertainties remain in BB factors, leading to large deviations (−2.7% to 41.0%) in estimates of the contribution of BB to PM_{2.5}. However, studies have demonstrated that LG also has non-BB sources. On the basis of the data obtained in this study and the reported levels of coal and biomass consumption in Shaanxi Province in 2019, LG emissions were carefully estimated. The contribution of BB in Xi'an to ambient PM_{2.5} was overestimated by 9.9–28.2% when non-biomass sources are considered. The results indicated that existing methods often overestimate LG emissions from BB and that the contribution from non-BB sources should not be ignored. Therefore, future studies must reevaluate the potential emission sources of LG and their ramifications for the original method of estimating the contribution of BB.

Highlights

The diagnostic ratios of levoglucosan /OC and arabitol/EC varied greatly in different fuel.

Different sources had an obvious impact on BB contribution estimation.

A certain overestimation of biomass burning exerted when using LG as a sole tracer.

Author Contributions: Data curation, K.H., X.W. and B.Z.; Investigation, K.H. and Y.Z.; Methodology, R.Z. and J.S.; Supervision, Z.S. and J.S.; Writing—original draft, K.H.; Writing—review & editing, Z.S., J.S. and K.H.; Conceptualization, Z.S.; Visualization, K.H. All authors have read and agreed to the published version of the manuscript.

Funding: This research was supported by the National Key R&D Program of China (2017YFC0212205), the Natural Science Foundation of China (21661132005), and a grant from SKLLQG, the Chinese Academy of Sciences (SKLLQG1919).

Acknowledgments: The authors acknowledge the support of Institute of Earth Environment, Chinese Academy of Sciences, Xi'an, China.

Conflicts of Interest: The authors declare no conflict of interest.

Appendix A

Table A1. Sampling information and combustion conditions.

Information	Coal Stove			Wood Stove			Heated Kang		
	Anthracitic Coal	Bituminous Coal	Briquettes	Corn Cob	Wood Branches	Wood Branches	Wood Block	Maize Straw	Wheat Straw
Number of Samples	4	4	4	4	4	4	4	4	4
Average sample quality/g	862	850	843	530	492	496	501	511	524
Average sampling time/min	79	70	71	27	32	32	31	25	26
Combustion Conditions	flaming burning	flaming burning	flaming burning	flaming burning	flaming burning	smoldering burning	smoldering burning	smoldering burning	smoldering burning

Appendix B. The Concentration of LG and Arabitol in Stove Calculated Method

The concentration of LG and arabitol in source can be calculated based on their EF and stove volume (15–25 L). Take LG as an example, and LG concentration can be calculated as follows:

$$\text{Con}_{\text{LG}} = \frac{\text{EF}_{\text{LG}} \times m_{\text{fuel}}}{V},$$

where Con_{LG} is the concentration of LG (ng/m^3), EF is the emission factor of fuel (ng/kg), m_{fuel} is the mass of the burned fuel (kg), and V is the stove volume (m^3).

In the previous study, we measured levoglucosan and arabitol in ambient $\text{PM}_{2.5}$ samples during summer and winter in Xi'an city, northwestern China. The results indicated that the mean concentration of levoglucosan and arabitol in winter is $268.5 \text{ ng}/\text{m}^3$ and $8.9 \text{ ng}/\text{m}^3$, respectively. Take anthracite as an example, and the stove volume is 20 L, the estimated LG concentration in fume is $6896 \text{ ng}/\text{m}^3$, which is much larger than the natural background.

References

- Duan, X.L.; Jiang, Y.; Wang, B.B.; Zhao, X.G.; Shen, G.F.; Cao, S.Z.; Huang, N.; Qian, Y.; Chen, Y.T.; Wang, L.M. Household fuel use for cooking and heating in China: Results from the first Chinese Environmental Exposure-Related Human Activity Patterns Survey (CEERHAPS). *Appl. Energy* **2014**, *136*, 692–703. [\[CrossRef\]](#)
- Tao, S.; Ru, M.Y.; Du, W.; Zhu, X.; Zhong, Q.R.; Li, B.G.; Shen, G.F.; Pan, X.L.; Meng, W.J.; Chen, Y.L.; et al. Quantifying the Rural Residential Energy Transition in China from 1992 to 2012 through a Representative National Survey. *Nat. Energy* **2018**, *3*, 567–573. [\[CrossRef\]](#)
- Zhao, N.; Zhang, Y.; Li, B.; Hao, J.; Chen, D.; Zhou, Y.; Dong, R. Natural Gas and Electricity: Two Perspective Technologies of Substituting Coal-Burning Stoves for Rural Heating and Cooking in Hebei Province of China. *Energy Sci. Eng.* **2019**, *7*, 120–131. [\[CrossRef\]](#)
- Eriksson, A.C.; Nordin, E.Z.; Nyström, R.; Pettersson, E.; Swietlicki, E.; Bergvall, C.; Westerholm, R.; Boman, C.; Pagels, J.H. Particulate PAH Emissions from Residential Biomass Combustion: Time-Resolved Analysis with Aerosol Mass Spectrometry. *Environ. Sci. Technol.* **2014**, *48*, 7143–7150. [\[CrossRef\]](#) [\[PubMed\]](#)
- Unosson, J.; Blomberg, A.; Sandström, T.; Muala, A.; Boman, C.; Nyström, R.; Westerholm, R.; Mills, N.L.; Newby, D.E.; Langrish, J.P.; et al. Exposure to wood smoke increases arterial stiffness and decreases heart rate variability in humans. *Part. Fibre Toxicol.* **2013**, *10*, 20. [\[CrossRef\]](#) [\[PubMed\]](#)

6. Jacobson, M.Z. Effects of biomass burning on climate, accounting for heat and moisture fluxes, black and brown carbon, and cloud absorption effects. *J. Geophys. Res. Atmos.* **2014**, *119*, 8980–9002. [[CrossRef](#)]
7. Kelly, F.J.; Fussell, J.C. Size, source and chemical composition as determinants of toxicity attributable to ambient particulate matter. *Atmos. Environ.* **2012**, *60*, 504–526. [[CrossRef](#)]
8. Chen, J.M.; Li, C.L.; Ristovski, A.; Milic, A.; Gu, Y.T.; Sislam, M.; Wang, S.X.; Hao, J.M.; Zhang, H.F.; He, C.R.; et al. A review of biomass burning: Emissions and impacts on air quality, health and climate in China. *Sci. Total Environ.* **2017**, *579*, 1000–1034. [[CrossRef](#)]
9. Pöschl, U. Atmospheric Aerosols: Composition, Transformation, Climate and Health Effects. *Angew. Chem.* **2005**, *44*, 7520–7540. [[CrossRef](#)]
10. Turpin, B.J.; Huntzicker, J.J. Identification of secondary organic aerosol episodes and quantitation of primary and secondary organic aerosol concentrations during SCAQS. *Atmos. Environ.* **1995**, *29*, 3527–3544. [[CrossRef](#)]
11. Bond, T.C.; Doherty, S.J.; Fahey, D.W.; Forster, P.M.; Berntsen, T.; DeAngelo, B.J.; Flanner, M.G.; Ghan, S.; Kärcher, B.; Koch, D.; et al. Bounding the role of black carbon in the climate system: A scientific assessment. *J. Geophys. Res. Atmos.* **2013**, *118*, 5380–5552. [[CrossRef](#)]
12. Watson, J.G.; Chow, J.C.; Houck, J.E. PM_{2.5} chemical source profiles for vehicle exhaust, vegetative burning, geological material, and coal burning in Northwestern Colorado during 1995. *Chemosphere* **2001**, *43*, 1141–1151. [[CrossRef](#)]
13. Saitoh, K.; Sera, K.; Hirano, K.; Shirai, T. Chemical characterization of particles in winter-night smog in Tokyo. *Atmos. Environ.* **2002**, *36*, 435–440. [[CrossRef](#)]
14. Geng, H.; Park, Y.; Hwang, H.; Kang, S.; Ro, C.U. Elevated nitrogen-containing particles observed in Asian dust aerosol samples collected at the marine boundary layer of the Bohai Sea and the Yellow Sea. *Atmos. Chem. Phys.* **2009**, *9*, 6933–6947. [[CrossRef](#)]
15. Tang, X.; Zhang, X.S.; Wang, Z.W.; Ci, Z.J. Water-soluble organic carbon (WSOC) and its temperature-resolved carbon fractions in atmospheric aerosols in Beijing. *Atmos. Res.* **2016**, *181*, 200–210. [[CrossRef](#)]
16. Taylor, N.F.; Collins, D.R.; Lowenthal, D.H.; Zielinska, B.; Samburova, V.; Kumar, N.; Hallar, A.G.; Mazzoleni, L.R.; Mccubbin, I.B. Hygroscopic growth of water soluble organic carbon isolated from atmospheric aerosol collected at US national parks and storm Peak Laboratory. *Atmos. Chem. Phys.* **2017**, *17*, 2555–2571. [[CrossRef](#)]
17. Xiang, P.; Zhou, X.M.; Duan, J.C.; Tan, J.H.; He, K.B.; Yuan, C.; Ma, Y.L.; Zhang, Y.X. Chemical characteristics of water-soluble organic compounds (WSOC) in PM_{2.5} in Beijing, China: 2011–2012. *Atmos. Res.* **2017**, *183*, 104–112. [[CrossRef](#)]
18. Fraser, M.P.; Lakshmanan, K. Using levoglucosan as a molecular marker for the long-range transport of biomass combustion aerosols. *Environ. Sci. Technol.* **2000**, *34*, 4560–4564. [[CrossRef](#)]
19. Ho, K.F.; Engling, G.; Ho, S.S.A.; Huang, R.J.; Lai, S.C.; Cao, J.J.; Lee, S.C. Seasonal variations of anhydrosugars in PM_{2.5} in the Pearl River Delta region, China. *Tellus B Chem. Phys. Meteorol.* **2014**, *66*, 22577. [[CrossRef](#)]
20. Bhattarai, H.; Saikawa, E.; Wan, X.; Zhu, H.X.; Kirpa, R.; Gao, S.P.; Kang, S.C.; Zhang, Q.Q.; Zhang, Y.L.; Wu, G.M.; et al. Levoglucosan as a tracer of biomass burning: Recent progress and perspectives. *Atmos. Res.* **2019**, *220*, 20–33. [[CrossRef](#)]
21. Fu, P.Q.; Kawamura, K.; Kobayashi, M.; Simoneit, B.R. Seasonal variations of sugars in atmospheric particulate matter from Gosan Jeju Island: Significant contributions of airborne pollen and Asian dust in spring. *Atmos. Environ.* **2012**, *55*, 234–239. [[CrossRef](#)]
22. Li, X.; Chen, M.; Le, H.P.; Wang, F.; Guo, Z.; Iinuma, Y.; Chen, J.; Herrmann, H. Atmospheric outflow of PM_{2.5} saccharides from megacity Shanghai to East China Sea: Impact of biological and biomass burning sources. *Atmos. Environ.* **2016**, *143*, 1–14. [[CrossRef](#)]
23. Salma, I.; Németh, Z.; Weidinger, T.; Maenhaut, W.; Claeys, M.; Molnár, M.; Major, I.; Ajtai, T.; Utry, N.; Bozóki, Z. Source apportionment of carbonaceous chemical species to fossil fuel combustion, biomass burning and biogenic emissions by a coupled radiocarbon–levoglucosan marker method. *Atmos. Chem. Phys.* **2017**, *17*, 13767–13781. [[CrossRef](#)]
24. Wang, Q.Q.; Shao, M.; Liu, Y.; William, K.; Paul, G.; Li, X.H.; Liu, Y.; Lu, S.H. Impact of biomass burning on urban air quality estimated by organic tracers: Guangzhou and Beijing as cases. *Atmos. Environ.* **2007**, *41*, 8380–8390. [[CrossRef](#)]
25. Yan, C.; Zheng, M.; Sullivan, A.P.; Bosch, C.; Desyaterik, Y.; Andersson, A.; Li, X.; Guo, X.; Zhou, T.; Gustafsson, O.; et al. Chemical characteristics and light-absorbing property of water-soluble organic carbon in Beijing: Biomass burning contributions. *Atmos. Environ.* **2015**, *121*, 4–12. [[CrossRef](#)]
26. Zhang, T.; Cao, J.J.; Chow, J.C.; Shen, Z.X.; Ho, K.F.; Steven, S.H.H.; Liu, S.X.; Han, Y.M.; John, G.W.; Wang, G.H. Characterization and seasonal variations of levoglucosan in fine particulate matter in Xi’an China. *J. Air. Waste Manage. Assoc.* **2014**, *64*, 1317–1327. [[CrossRef](#)]
27. Zhu, C.S.; Cao, J.J.; Tsai, C.J.; Zhang, Z.S.; Tao, J. Biomass burning tracers in Rural and urban ultrafine particles in Xi’an China. *Atmos. Pollution Res.* **2017**, *8*, 614–618.
28. Harrison, R.M.; Beddows, D.C.S.; Hu, L.; Yin, J. Comparison of methods for evaluation of wood smoke and estimation of UK ambient concentrations. *Atmos. Chem. Phys.* **2012**, *12*, 8271–8283. [[CrossRef](#)]
29. Zhang, T.; Claeys, M.; Cachier, H.; Dong, S.; Wang, W.; Maenhaut, W.; Liu, X. Identification and estimation of the biomass burning contribution to Beijing aerosol using levoglucosan as a molecular marker. *Atmos. Environ.* **2008**, *42*, 7013–7021. [[CrossRef](#)]
30. Wang, X.; Shen, Z.X.; Zeng, Y.; Liu, F.; Zhang, Q.; Lei, Y.; Xu, H.; Cao, J.; Yang, L. Day-Night differences, Seasonal Variations and Source Apportionment of PM₁₀-Bound PAHs over Xi’an, Northwest China. *Atmosphere* **2018**, *9*, 62. [[CrossRef](#)]

31. Yan, C.; Zheng, M.; Sullivan, A.P.; Shen, G.; Chen, Y.; Wang, S.; Zhao, B.; Cai, S.; Desyaterik, Y.; Li, X. Residential coal combustion as a source of levoglucosan in China. *Environ. Sci. Technol.* **2018**, *52*, 1665–1674. [[CrossRef](#)]
32. Wu, J.; Kong, S.; Zeng, X.; Cheng, Y.; Qi, S. First high-resolution emission inventory of levoglucosan for biomass burning and non-biomass burning sources in China. *Environ. Sci. Technol.* **2021**, *55*, 1497–1507. [[CrossRef](#)] [[PubMed](#)]
33. Kourtchev, I.; Hellebust, S.; Bell, J.M.; O'Connor, I.P.; Healy, R.M.; Allanic, A.; Healy, D.; Wenger, J.C.; Sodeau, J.R. The use of polar organic compounds to estimate the contribution of domestic solid fuel combustion and biogenic sources to ambient levels of organic carbon and PM_{2.5} in Cork Harbour, Ireland. *Sci. Total Environ.* **2011**, *409*, 2143–2155. [[CrossRef](#)] [[PubMed](#)]
34. Fabbri, D.; Marynowski, L.; Fabianska, M.J.; Zaton, M.; Simoneit, B.R.T. Levoglucosan and other cellulose markers in pyrolysates of miocene lignites: Geochemical and environmental implications. *Environ. Sci. Technol.* **2008**, *42*, 2957–2963. [[CrossRef](#)] [[PubMed](#)]
35. Fabbri, D.; Torri, C.; Simoneit, B.R.T.; Marynowski, L.; Rushdi, A.I.; Fabianska, M.J. Levoglucosan and other cellulose and lignin markers in emissions from burning of Miocene lignites. *Atmos. Environ.* **2009**, *43*, 2286–2295. [[CrossRef](#)]
36. Rybicki, M.; Marynowski, L.; Simoneit, B.R.T. Composition of organic compounds from low-temperature burning of lignite and their application as tracers in ambient air. *Chemosphere* **2020**, *249*, 126087. [[CrossRef](#)] [[PubMed](#)]
37. Shen, Z.X.; Han, Y.M.; Cao, J.J.; Jing, T.; Zhu, C.S.; Liu, P.P.; Wang, Y.Q. Characteristics of traffic-related emissions: A case study in roadside ambient air over Xi'an, China. *Aerosol Air Qual. Res.* **2010**, *10*, 292–300. [[CrossRef](#)]
38. Cao, J.J.; Shen, Z.X.; Chow, J.C.; Watson, J.G.; Lee, S.C.; Tie, X.X.; Ho, K.F.; Wang, G.H.; Han, Y.M. Winter and summer PM_{2.5} chemical compositions in fourteen Chinese cities. *J. Air Waste Manag. Assoc.* **2012**, *62*, 1214–1226. [[CrossRef](#)]
39. Sun, J.; Shen, Z.X.; Cao, J.J.; Zhang, L.; Wu, T.; Zhang, Q.; Yin, X.; Huang, Y.; Huang, R.J. Particulate matters emitted from maize straw burning for winter heating in rural areas in Guanzhong Plain, China: Current emission and future reduction. *Atmos. Res.* **2017**, *184*, 66–76. [[CrossRef](#)]
40. Chow, J.C.; Watson, J.G.; Chen, L.W.A.; Chang, M.O.; Robinson, N.F.; Trimble, D.; Kohl, S. The IMPROVE_A temperature protocol for thermal/optical carbon analysis: Maintaining consistency with a long-term database. *J. Air Waste Manag. Assoc.* **2007**, *57*, 1014–1023. [[CrossRef](#)]
41. Shen, Z.X.; Cao, J.J.; Liu, S.; Zhu, C.; Wang, X.; Zhang, T.; Xu, H.; Hu, T. Chemical composition of PM₁₀ and PM_{2.5} collected at ground level and 100 meters during a strong winter-time pollution episode in Xi'an, China. *J. Air Waste Manag. Assoc.* **2011**, *61*, 1150–1159. [[CrossRef](#)] [[PubMed](#)]
42. Sun, J.; Shen, Z.X.; Zeng, Y.L.; Niu, X.Y.; Wang, J.H.; Cao, J.J.; Gong, X.S.; Xu, H.M.; Wang, T.B.; Liu, H.X.; et al. Characterization and cytotoxicity of PAHs in PM_{2.5} emitted from residential solid fuel burning in the Guanzhong Plain, China. *Environ. Pollut.* **2018**, *241*, 359–368. [[CrossRef](#)] [[PubMed](#)]
43. Naxieli, S.L.R.; Griselda, G.C.; José, J.F.L.; Mirella, G.A.; Claudia, O.V.; Irma, F.R.H.; Violeta, M.A. Emission factors of atmospheric and climatic pollutants from crop residues Burning. *J. Air Waste Manag. Assoc.* **2018**, *68*, 849–865.
44. Daniela, A.F.; Karla, M.L.; Turibio, G.S.N.; José, C.S.; Saulo, R.F.; Bernardo, F.T.R.; Ely, V.C.; Edson, A.; João, A.C.J. Pre-Harvest Sugarcane Burning: Determination of Emission Factors through Laboratory Measurements. *Atmosphere* **2012**, *3*, 164–180.
45. Sun, J.; Shen, Z.X.; Zhang, Y.; Zhang, Q.; Wang, F.R.; Wang, T.; Chang, X.J.; Lei, Y.L.; Xu, H.M.; Cao, J.J.; et al. Effects of biomass briquetting and carbonization on PM_{2.5} emission from residential burning in Guanzhong Plain, China. *Fuel* **2019**, *244*, 379–387. [[CrossRef](#)]
46. Chen, Y.J.; Zhi, G.R.; Feng, Y.L.; Fu, J.; Feng, J.; Sheng, G.; Simoneit, B.R.T. Measurements of emission factors for primary carbonaceous particles from residential raw-coal combustion in China. *Geophys. Res. Lett.* **2006**, *33*, 20. [[CrossRef](#)]
47. Shen, G.F.; Yang, Y.; Wang, W.; Tao, S.; Zhu, C.; Min, Y.; Xue, M.; Ding, J.; Wang, B.; Wang, R. Emission factors of particulate matter and elemental carbon for crop residues and coals burned in typical household stoves in China. *Environ. Sci. Technol.* **2010**, *44*, 7157–7162. [[CrossRef](#)] [[PubMed](#)]
48. Li, X.; Wang, S.; Duan, L.; Hao, J.M. Characterization of non-methane hydrocarbons emitted from open burning of wheat straw and corn stover in China. *Environ. Res. Lett.* **2009**, *4*, 4. [[CrossRef](#)]
49. Ni, H.; Han, Y.; Cao, J.J.; Chen, L.W.; Tian, J.; Wang, X.L.; Chow, J.C.; Watson, J.G.; Wang, Q.Y.; Wang, P.; et al. Emission characteristics of carbonaceous particles and trace gases from open burning of crop residues in China. *Atmos. Environ.* **2015**, *123*, 399–406. [[CrossRef](#)]
50. Akagi, S.K.; Yokelson, R.J.; Wiedinmyer, C.; Alvarado, M.J.; Reid, J.S.; Karl, T.; Crouse, J.D.; Wennberg, P.O. Emission factors for open and domestic biomass burning for use in atmospheric models. *Atmos. Chem. Phys.* **2011**, *11*, 4039–4072. [[CrossRef](#)]
51. Trubetskaya, A.; Lin, C.; Ovadnevaite, J.; Ceburnis, D.; O'Dowd, C.; Leahy, J.J.; Monaghan, R.F.D.; Johnson, R.; Layden, P.; Smith, W. Study of Emissions from Domestic Solid-Fuel Stove Combustion in Ireland. *Energy Fuels* **2021**, *35*, 4966–4978. [[CrossRef](#)]
52. Shen, G.F.; Chen, Y.; Xue, C.; Lin, N.; Huang, Y.; Shen, H.; Wang, Y.; Li, T.; Zhang, Y.; Su, S. Pollutant emissions from improved coal-and wood-fuelled cookstoves in rural households. *Environ. Sci. Technol.* **2015**, *49*, 6590–6598. [[CrossRef](#)] [[PubMed](#)]
53. Zhi, G.R.; Chen, Y.J.; Feng, Y.L.; Xiong, S.C.; Li, J.; Zhang, G.; Sheng, G.Y.; Fu, J.M. Emission characteristics of carbonaceous particles from various residential coal-stoves in China. *Environ. Sci. Technol.* **2008**, *42*, 3310–3315. [[CrossRef](#)]
54. Lei, Y.L.; Shen, Z.X.; Zhang, T.; Wang, Q.; Sun, J.; Gong, X.; Cao, J.J.; Xu, H.M.; Liu, S.X. Optical source profiles of brown carbon in size-resolved particulate matter from typical domestic biofuel burning over Guanzhong Plain, China. *Sci. Total Environ.* **2018**, *622*, 244–251. [[CrossRef](#)] [[PubMed](#)]
55. Hays, M.D.; Fine, P.M.; Geron, C.D.; Kleeman, M.J.; Gullett, B.K. Open burning of agricultural biomass: Physical and chemical properties of particle-phase emissions. *Atmos. Environ.* **2005**, *39*, 6747–6764. [[CrossRef](#)]

56. Sillapapiromsuk, S.; Chantara, S.; Tengjaroenkul, U.; Prasitwattanaseree, S.; Prapamontol, T. Determination of PM10 and its ion composition emitted from biomass burning in the chamber for estimation of open burning emissions. *Chemosphere* **2013**, *93*, 1912–1919. [[CrossRef](#)]
57. Shen, Z.X.; Cao, J.J.; Arimoto, R.; Han, Z.; Zhang, R.; Han, Y.; Liu, S.X.; Okuda, S.; Nakao, S.; Tanaka, S. Ionic composition of TSP and PM 2.5 during dust storms and air pollution episodes at Xi'an, China. *Atmos. Environ.* **2009**, *43*, 2911–2918. [[CrossRef](#)]
58. Li, X.H.; Wang, S.X.; Duan, L.; Hao, J.M.; Nie, Y.F. Carbonaceous aerosol emissions from household biofuel combustion in China. *Environ. Sci. Technol.* **2009**, *43*, 6076–6081. [[CrossRef](#)]
59. Huang, R.J.; Zhang, Y.; Bozzetti, C.; Ho, K.F.; Cao, J.J.; Han, Y.; Daellenbach, K.R.; Slowik, J.G.; Platt, S.M.; Canonaco, F.; et al. High secondary aerosol contribution to particulate pollution during haze events in China. *Nature* **2014**, *514*, 218–222. [[CrossRef](#)] [[PubMed](#)]
60. Fine, P.M.; Cass, G.R.; Simoneit, B.R. Chemical characterization of fine particle emissions from fireplace combustion of woods grown in the northeastern United States. *Environ. Sci. Technol.* **2001**, *35*, 2665–2675. [[CrossRef](#)] [[PubMed](#)]
61. Lindberg, D.; Niemi, J.; Engblom, M. Effect of temperature gradient on composition and morphology of synthetic chlorine-containing biomass boiler deposits. *Fuel. Process. Technol.* **2016**, *141*, 285–298. [[CrossRef](#)]
62. Zhang, Z.; Jian, G.; Engling, G.; Tao, J.; Chai, F.; Zhang, L.; Zhang, R.; Sang, X.; Chan, C.Y.; Lin, Z. Characteristics and applications of size-segregated biomass burning tracers in China's Pearl River Delta region. *Atmos. Environ.* **2015**, *105*, 290–301. [[CrossRef](#)]
63. Xu, H.M.; Cao, J.J.; Gao, M.L.; Ho, K.F.; Niu, X.Y.; Coons, T.L.; Steven, S.H.H.; Wang, G.H.; Zhao, Z. Personal exposure to fine particulates and polycyclic aromatic hydrocarbons in an office environment in Xi'an, China. *Front. Env. Sci. Eng.* **2013**, *2*, 33–46.
64. Zhang, Y.; Tian, J.; Shen, Z.; Wang, W.; Ni, H.; Liu, S.; Cao, J. Emission Characteristics of PM2.5 and Trace Gases from Household Wood Burning in Guanzhong Plain, Northwest China. *Aerosol Sci. Eng.* **2018**, *2*, 130–140. [[CrossRef](#)]